

Evidence for the Development of a One-Dimensional Array of Crystallites in Stretched Polyaniline and the Effect of Cl⁻ Doping

B. K. Annis^{*,†} and J. S. Lin^{*,‡}

Chemistry Division and Solid State Division, Oak Ridge National Laboratory,
P.O. Box 2008, Oak Ridge, Tennessee 37831-6197

E. M. Scherr and A. G. MacDiarmid

Department of Chemistry, University of Pennsylvania,
Philadelphia, Pennsylvania 19104-6323

Received November 14, 1990; Revised Manuscript Received August 16, 1991

ABSTRACT: Small-angle X-ray scattering data obtained from drawn films of the emeraldine base form of polyaniline indicate the development of an array of crystalline regions which is periodic along the draw axis. The spacing is 16 ± 3 nm and the extent of the crystallites is about 6 nm. Doping the films with Cl⁻ appears to reduce the electron density of the crystalline regions and eliminates this source of scattering.

Introduction

The drawing or stretching of polymers has often been used to enhance physical properties of technological interest such as tensile strength and more recently electrical conductivity.¹⁻⁴ The processing invariably results in structural changes at various levels, and it is of interest to determine these changes and, if possible, correlate them with the property of interest. As a contribution toward this end, small-angle X-ray scattering (SAXS) observations which provide information on a scale of 5–100 nm have been obtained for films of drawn emeraldine and the conducting salt formed by subsequent doping with Cl⁻. The origins of SAXS are spatial fluctuations in the electron density which are typically identified with the presence of scattering entities such as microvoids, fibrils, and crystallites. Supplementary measurements are often necessary to determine the nature of the scattering entities, and here, wide-angle X-ray scattering was used to verify the presence of a crystalline phase.

Experimental Section

A 2% solution (w/w) of emeraldine base ($[-\text{NHC}_6\text{H}_4-\text{NHC}_6\text{H}_4\text{N}=\text{C}_6\text{H}_4-\text{NC}_6\text{H}_4-]_x$) in *N*-methyl-2-pyrrolidinone (NMP, Aldrich Chemical, 99%) was made by slowly adding 20 g of finely ground emeraldine base powder to 1 L of NMP which was magnetically stirred. Approximately 250 mL of this solution was poured onto a clean 8 in. \times 15 in. sheet of glass. Two of these coated glass sheets were placed in a vacuum oven (Fisher Isotemp) at $\sim 50^\circ\text{C}$ for ~ 24 h.

After the films had dried they were removed from the glass by immersion in distilled water and peeled off. The film was cut into 1.5-in. wide strips 15 in. long. Each strip was threaded through a uniaxial web stretching device (Foster-Miller Co.)⁵ where it contacted two heated rollers. The first roller is where the stretching takes place; it was set at $148 \pm 2^\circ\text{C}$, as confirmed by a thermocouple. The second heated roller is used for annealing the sample, and it was set at $100 \pm 2^\circ\text{C}$. Stretching ratios are controlled by varying the speeds of the pinch rollers as the film is fed through the device. The samples were made of carefully aligned stacks of the films which were typically 10 μm thick.

The SAXS experiments were done with the Oak Ridge National Laboratory SAXS facility⁶ which makes use of a rotating anode X-ray source (Cu K α), pinhole collimation and a two-dimensional position sensitive detector (20 \times 20 cm). Various angular ranges are obtained by changing the sample to detector position and,

for this work, distances of 2 and 5 m were used. Absolute intensities were obtained by calibration with a polyethylene standard.⁷ The corresponding range in the scattering momentum transfer $k = (4\pi/\lambda) \sin(\theta_{\text{cat}}/2)$ was 0.04–1.5 nm⁻¹. The wide-angle photographs were obtained with a standard flat film X-ray camera which used Ni filtered Cu radiation.

Discussion

For randomly oriented scattering entities the isointensity contours of the scattered radiation are in the form of concentric rings. The scattering from a sample with a draw ratio of 2 showed no significant deviation from this pattern, and the magnitude of the scattering was also not significantly different from an unstretched sample. This was not the case for a sample with a draw ratio of 2.5, as may be seen in Figure 1a. The isointensity contours in the central portion (corresponding to the smallest scattering angles and largest dimensions) are roughly elliptical with a major axis parallel to the draw direction. Due to the reciprocal nature of scattering this type of contour indicates the presence of scattering entities elongated perpendicular to the draw axis. This feature was also found in emeraldine films drawn under somewhat different conditions.⁴ As the scattering angle increases the major axis of the contours becomes perpendicular to the draw axis and implies the presence of scattering entities elongated parallel to the draw axis. The latter feature is quite common in drawn polymers and is frequently attributed to voids which have been stretched parallel to the axis. These voids can take the form of elongated cavities in an otherwise structureless matrix or can be the empty spaces occurring in a mat of partially oriented fibrils which are disperse in diameter. The available information does not permit distinguishing between these possibilities. The superposition of scattering entities indicated in Figure 1a is somewhat less common but has been observed before in other polymers (e.g. ref 8) and may be associated with the onset of crazing.⁹ The wide-angle X-ray scattering from the sample is shown in Figure 2a and is similar to that observed for stretched amorphous polymers.¹⁰ On this basis there is no reason to attribute the SAXS observations to the presence of crystallites. SAXS data were also obtained on a sample with a draw ratio of 3, and the contour plot was found to be quite similar to Figure 1a.

There is no obvious way to unequivocally separate the contributions from the two types of scattering entities

[†] Chemistry Division.

[‡] Solid State Division.

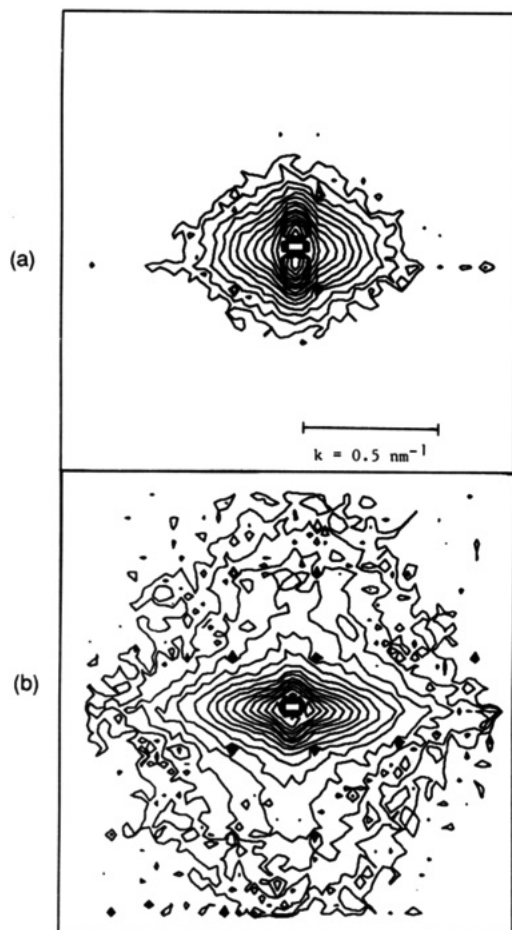


Figure 1. (a) Isointensity contours for undoped sample with a draw ratio of 2.5. Apparatus was in 5-m configuration. This and all subsequent plots represent data which have been corrected for detector sensitivity, background, and transmission. The minimum and maximum contours are the same for all plots. Draw axis is vertical. (b) Results for undoped sample with draw ratio of 4.

and obtain the characteristic dimensions of each parallel and perpendicular to the draw axis. However, a qualitative estimate of an average dimension is provided by applying the usual Guinier analysis¹¹ to an azimuthal average of the data. In this analysis, at the smallest angles, the scattering intensity is given by

$$I = I(0) \exp(-(kR_g)^2/3) \quad (1)$$

and the radius of gyration (R_g) may be obtained from the slope of a plot of the log of the intensity versus k^2 . In this manner an estimate of 20–25 nm was obtained for R_g . In the approximation of a spherical scattering entity this implies a diameter of approximately 50 nm.

The isointensity contour plot for a sample with a draw ratio of 4 is shown in Figure 1b. Here also the central portion of the plot indicates scattering from a superposition of entities oriented parallel and perpendicular to the draw axis. Figure 3 indicates that meridional (parallel to the draw axis) intensity slices for the samples drawn 2.5 \times and 4 \times are quite similar in the core region. The shapes of the equatorial slices were also found to be similar. The equatorial slice for the sample with a draw ratio of 4 is shown in Figure 4. No structure is noticeable in the equatorial slice (Figure 4) which implies that no new type of scattering element contributes to the scattering in this direction.

From Figure 1b it is quite apparent that this is not the case for scattering at larger angles along the meridional

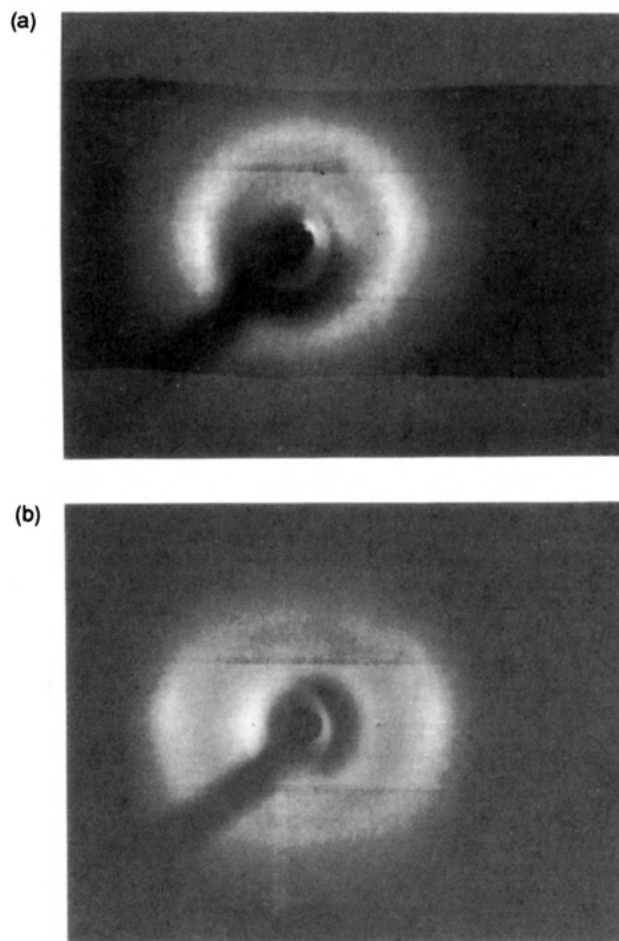


Figure 2. (a) Wide-angle pattern for undoped sample with draw ratio of 2.5; draw axis is vertical; approximate range in 2θ is 40° . (b) Same for doped sample drawn 2.5 \times .

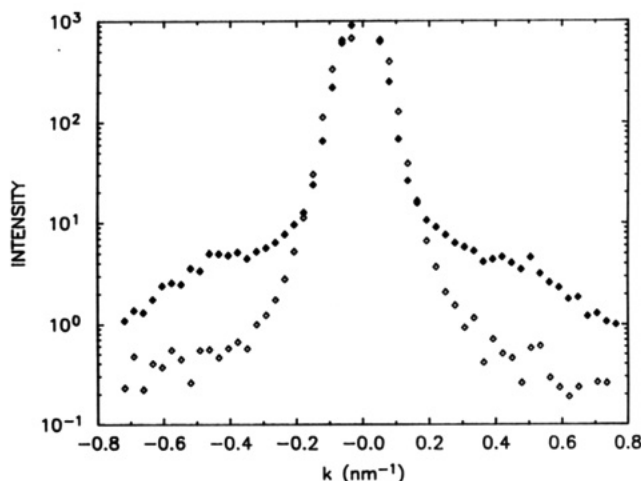


Figure 3. Meridional intensity slices in absolute units of cross section per unit volume (cm^{-1}), 2.5 \times (\diamond) and 4 \times (\blacklozenge) samples, 5-m configuration.

direction. Quite distinct lobes have developed in the contour plot and correspond to the shoulders evident in Figures 3 and 5. Patterns analogous to Figure 1b have frequently been observed for drawn partially crystalline polymers (e.g. refs 12 and 13), and the wide-angle scattering pattern shown in Figure 6a provides a clear indication that crystalline regions are present in this sample. The SAXS data indicate that these regions have a periodicity along the draw axis. The lobes were also observed for a sample with a draw ratio of 3.5, and a wide-angle pattern similar to Figure 6a was observed as well. In the ideal case

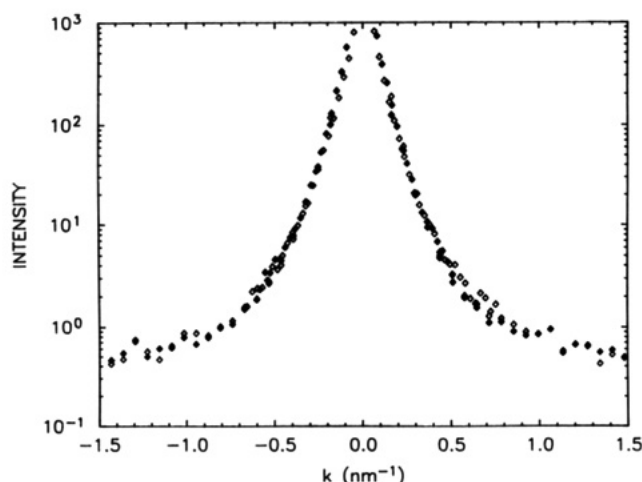


Figure 4. Equatorial slice for doped (\blacklozenge) and undoped sample (\diamond) with draw ratio of 4. Data from 2- and 5-m apparatus configurations have been combined.

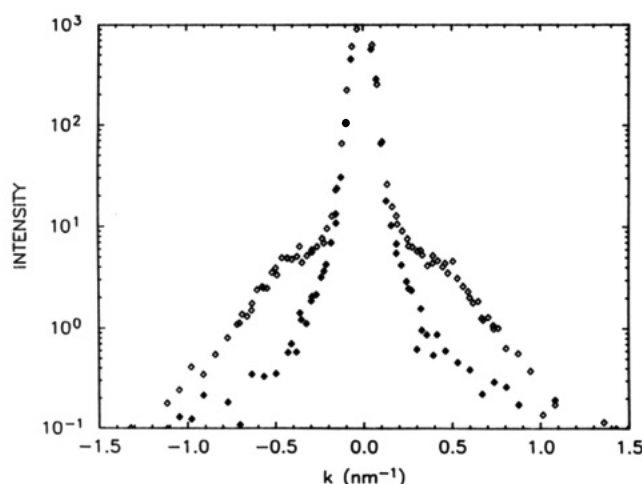


Figure 5. Meridional slices for doped (\blacklozenge) and undoped (\diamond) sample drawn 4 \times . Data from 2- and 5-m configurations have been combined.

the lobes along the meridian would be well separated from the scattering at smaller angles and the so-called long period, between the crystalline regions, can readily be estimated from Bragg's law ($d = 2\pi/k_{\text{max}}$, where k_{max} is the position of maximum intensity). Here the intense scattering at the smallest angles introduces an element of uncertainty as to the exact peak location; however, from Figure 3, a value of $k = 0.4 \pm 0.08 \text{ nm}^{-1}$ appears to be appropriate. This gives a spacing of $16 \pm 3 \text{ nm}$. The lack of any similar feature in the equatorial slice suggests that there is no significant correlation between crystalline regions in this direction. An extensive effort was made to improve the estimate of the spacing through the use of the paracrystalline model developed by Hosemann and co-workers.¹² However, no acceptable fit could be found that would cover the region of smallest angles below the shoulder. This reinforces the suggestion that the scattering is due to more than one source.

A standard Scherrer peak width analysis¹⁴ of diffractometer traces through the first two equatorial peaks and the meridional peak of Figure 6a produced a value of 6–7 nm for both directions. This similarity in the dimensions is in accord with the general appearance of the lobes in the contour plot (Figure 1b) in the sense that the extent in the two directions is much the same. For comparison, the dimensions for the crystallites are similar to those obtained from the SAXS analysis of drawn polypropylene^{12b} and

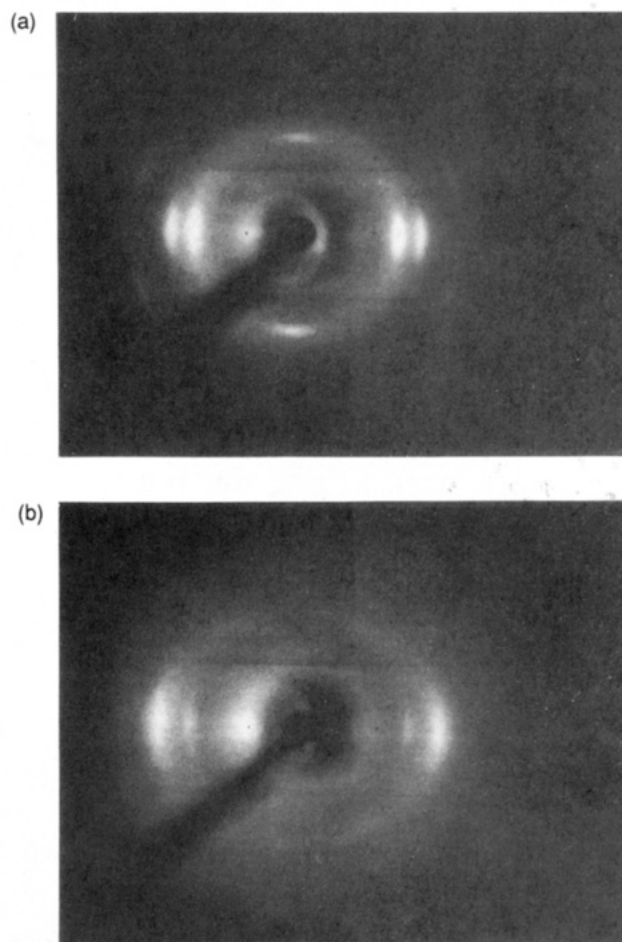


Figure 6. (a) Wide-angle pattern for undoped sample with draw ratio of 4; draw axis is vertical; approximate range in 2θ is 40° . (b) Same for doped sample drawn 4 \times .

Nylon 6.¹⁵ The diameter compares well with the 5-nm value obtained by Pouget et al.¹⁶ by wide-angle scattering from an emeraldine film with a draw ratio of 3. However, a value of 15 nm was obtained for the dimension parallel to the draw axis in that work. The difference in the estimates of the crystallite sizes could indicate that the crystallization is sensitive to the details of the processing.

The structural changes brought about by doping the emeraldine films to produce the conducting HCl salt form are of interest in an ongoing effort to understand and improve the electrical properties of the material. Consequently, when the measurements were completed, the samples were doped in 1 M HCl to the maximum [Cl]/[N] ratio of 0.5. The SAXS and wide-angle measurements were then repeated. In the case of the sample drawn 2.5 \times little difference is apparent in the isointensity contour plot (Figure 7a). In addition the radii of gyration were not affected outside experimental uncertainty (10%).

The effect of doping the sample with a draw ratio of 4 was also relatively little at the smallest scattering angles, but as can be seen in Figures 5 and 7b, the lobes along the meridian have disappeared. The latter requires that the regions of different electron density arrayed along the draw axis are no longer present. This could occur by increasing the electron density of the amorphous regions or decreasing that of the crystalline regions. Flotation measurements on "X-ray amorphous" samples of doped films indicate that the density approaches that of the undoped crystalline material (as calculated from the unit cell data of Moon et al. (0.419 nm^3)¹⁷ and Pouget et al. (0.450 nm^3)).¹⁶ Consequently, the contrast originally causing the scattering

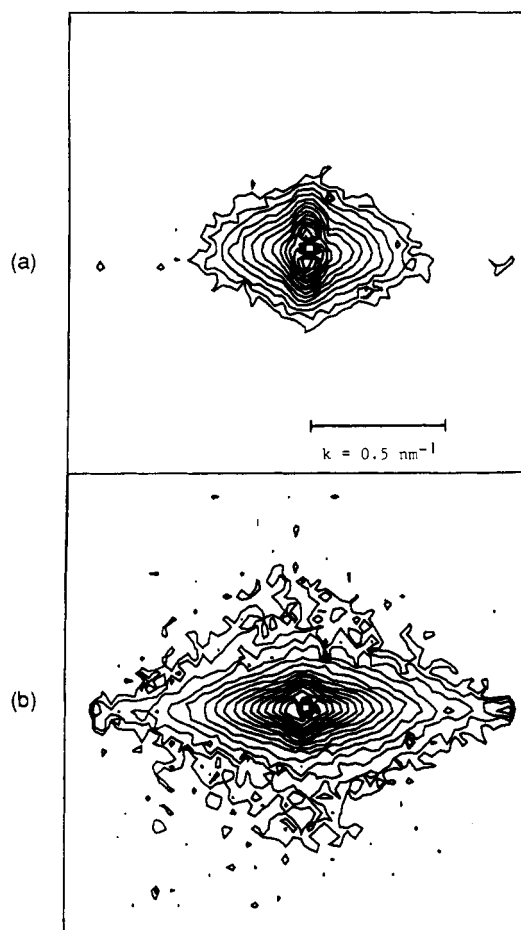


Figure 7. (a) Isointensity contours for sample drawn 2.5 \times and doped. Draw axis is vertical. (b) Isointensity contours for sample drawn 4 \times and doped. Draw axis is vertical.

would be reduced if the amorphous regions were to preferentially take up the Cl^- ions. However, the wide-angle scattering pattern Figure 6b does not resemble a superposition of structures with a contribution from undoped crystallites. Therefore, it would appear that the electron density of the crystalline regions is reduced by the doping. This is consistent with the rather surprising observation of Pouget et al.¹⁶ that the unit cell volume (0.585 nm^3) of the salt obtained from doped and stretched NMP cast film increases substantially more than would be expected from the introduction of Cl^- ions.

The observation that the doping has a significant effect only on a feature that can be correlated with the presence of crystallites substantiates the suggestion that the scattering from the undoped samples at the smallest angles and along the equatorial axis at wider angles (Figure 1, parts a and b) is not due to crystallites. In addition the 6-nm crystallite dimension found from the wide-angle scattering is too small to account for this scattering. On the assumption that this scattering is due to voids, an estimate, albeit a crude one, of the volume fraction can be obtained from the scattering invariant relation¹¹

$$\phi_v(1 - \phi_v) = (2\pi^3 R_T^2 \rho^2)^{-1} \int I(\vec{k}) d\vec{k} \quad (4)$$

where ρ is the electron density of the solid, R_T is the Thomson electron radius and ϕ_v is the volume fraction of the voids. This is valid only for a two-phase system, and the approximation is made that the scattering is significantly affected by crystallites only for k greater than 0.25 nm^{-1} . The mass density of several emeraldine base films has been determined by flotation to be $1.22 \pm 0.02 \text{ g/cm}^3$.

When the integral is approximated by a spherical average and use is made of the Porod tail model¹⁸ for the scattering at large angles, an estimate for the volume fraction of 0.002 attributed to voids results for the sample with a draw ratio of 4. This is roughly a factor of 20 times greater than that for the sample with a draw ratio of 2. The radius of gyration for the azimuthal average of the scattering at the smallest angles implies a diameter of approximately 50 nm and this varies only by about 15% as the draw ratio is changed. This indicates that the volume fraction increases principally by a change in the number density. The possibility that the scattering arises from particles of foreign matter whose population can increase with draw ratio and are of this size seems remote.

Conclusions

Under the prescribed conditions, drawing a film of polyaniline in the emeraldine base form can induce an array of crystalline regions with a degree of periodicity along the draw axis. No evidence of spatial correlation perpendicular to the axis was found. Doping the material with Cl^- causes a homogenization of electron density so that the periodicity, if indeed it still exists, is no longer readily observable by small-angle X-ray scattering. The wide-angle scattering for the doped material became more diffuse but suggested that some degree of crystallinity is still present, and it would seem unlikely that the periodicity is completely destroyed. An unfortunate conclusion which can be drawn from the results is that SAXS is unlikely to be a useful tool for monitoring the disposition of crystallites in doped versions of the polymer.

Initial infrared and UV-visible spectroscopic measurements¹⁹ on the doped, unstretched films have found anisotropic optical constants which vary with the stretch ratio. However, there is no indication that appearance of periodicity in the SAXS data for ratios greater than 3 is related to the variation of these constants.

In the case of the doped, stretched polymer anisotropy has been observed in the temperature dependence of the DC conductivity and the dielectric constant and it has been suggested that the behavior is in accord with a model in which the size of the crystallite regions is of importance rather than the magnitude and nature of the intercrystalline spacing.²⁰ Consequently, at this time it is not clear what the role of a residual periodicity in the doped polymer might be.

Acknowledgment. This research is sponsored by the Division of Materials Sciences, Office of Basic Energy Sciences, U.S. Department of Energy under contract DE-AC05-84OR21400 with the Martin Marietta Energy Systems, Inc. Work at the University of Pennsylvania was supported in part by the Defense Advanced Research Projects Agency through a contract monitored by the Office of Naval Research. The authors are grateful to Professor A. J. Epstein for conversations regarding the recent results contained in refs 19 and 20.

References and Notes

- Ogasawara, M.; Funahashi, K.; Demura, T.; Hagiwara, T.; Iwata, K. *Synth. Met.* 1986, 14, 61.
- Gagnon, D. R.; Karasz, F. E.; Thomas, E. L.; Lenz, R. W. *Synth. Met.* 1987, 20, 85.
- Naarman, H.; Theophilou, N. *Synth. Met.* 1987, 22, 1.
- (a) Theophilou, N.; MacDiarmid, A. G.; Annis, B. K.; Epstein, A. J. *Bull. Am. Phys. Soc.* 1989, 34, 583. (b) Annis, B. K.; Specht, E. D.; Theophilou, N.; MacDiarmid, A. G. *Polymer* 1991, 32, 1160. (c) Fischer, J. E.; Cajipe, V. B.; Zhu, Q.; Tang, X.; Scherr, E. M.; McGhie, A. R.; MacDiarmid, A. G. *Bull. Am. Phys. Soc.* 1991, 36, 624.

- (5) Machado, J. M.; Karasz, F. E.; Kovar, R. F.; Burnett, J. M.; Druy, M. A. *New Polymeric Mater.* **1989**, *1*, 189.
- (6) Wignall, G.; Lin, J. S.; Spooner, S. *J. Appl. Cryst.*, in press.
- (7) Hendricks, R. W. *J. Appl. Cryst.* **1978**, *11*, 15.
- (8) Russell, T. P.; Lin, J. S.; Spooner, S.; Wignall, G. D. *J. Appl. Cryst.* **1988**, *21*, 629.
- (9) (a) Statton, W. O. *Newer Methods of Polymer Characterization*; Ke, B. Ed.; Interscience Publishers: New York, 1964. (b) Garton, A.; Stepniak, R. F.; Carlsson, D. J.; Wiles, D. M. *J. Polym. Sci. Polym. Phys. Ed.* **1978**, *16*, 599.
- (10) (a) Brown, H. R.; Kramer, E. J. *Macromol. Sci. Phys.* **1981**, *B19*, 487. (b) Dettenmaier, M. *Advances in Polymer Science* 52/53, *Crazing in Polymers*; Kavsich, H. H. Ed.; Springer-Verlag: Berlin, 1983; p 57.
- (11) Alexander, L. E. *X-ray Diffraction Methods in Polymer Science*, Wiley-Interscience: New York, 1969; p 386.
- (12) Guinier, A.; Fournet, G. *Small-Angle Scattering of X-rays*; John Wiley and Sons: New York, 1955.
- (13) (a) Hosemann, R.; Bagchi, S. N. *Direct Analysis of Diffraction by Matter*; North-Holland, Amsterdam, 1962. (b) Ferracini, A.; Ferrero, A. J. *Macromol. Sci. Phys.* **1974**, *B10*, 97. (c) Cacković, J.; Loboda, J.; Hosemann, R. and Cacković, H.; Ferrero, F.; Ferracini, E. *Polymer* **1976**, *17*, 303. (d) Rognoni, A.; Ferrero, A.; Ferracini, E.; Cacković, J.; Loboda, J. *J. Polym. Sci., Polym. Phys. Ed.* **1984**, *22*, 485.
- (14) Chuah, H. H.; Lin, J. S.; Porter, R. S. *Macromolecules* **1986**, *19*, 2732.
- (15) Schultz, J. M. *Diffraction for Materials Scientists*; Prentice-Hall, Inc.: Englewood Cliffs, 1982; p 226.
- (16) Ferracini, E.; Ferrero, A. *Makromol. Chem.* **1988**, *189*, 1957.
- (17) Pouget, J. P.; Józefowicz, M. E.; Epstein, A. J.; Tang, X.; MacDiarmid, A. G. To be published.
- (18) Moon, Y. B.; Cao, Y.; Smith, P. and Heeger, A. J. *Polym. Commun.* **1984**, *30*, 196.
- (19) Porod, G. *Kolloid-Z.* **1951**, *124*, 83.
- (20) Cromack, K. R.; Józefowicz, M. E.; Ginder, J. M.; McCall, R. P.; Du, G.; Kim, K.; Li, C.; Wang, Z.; Epstein, A. J.; Druy, M. A.; Glatkowski, P. J.; Scherr, E. M.; MacDiarmid, A. G. To be published.
- (21) Wang, Z. H.; Li, C.; Epstein, A. J.; Scherr, E. M.; MacDiarmid, A. G. To be published.

Registry No. (C₆H₇N)_x (homopolymer), 25233-30-1; (C₆H₇N)_x·xHCl (homopolymer), 89183-45-9.